Blue channel of the Keck low-resolution imaging spectrometer

James K. McCarthy, Judith G. Cohen, Brad Butcher, John Cromer, Ernest Croner, et al.

James K. McCarthy, Judith G. Cohen, Brad Butcher, John Cromer, Ernest Croner, William R. Douglas Jr., Richard M. Goeden, Tony Grewal, Barry Lu, Harold L. Petrie, Tianxiang Weng, Bob Weber, Donald G. Koch, J. Michael Rodgers, "Blue channel of the Keck low-resolution imaging spectrometer," Proc. SPIE 3355, Optical Astronomical Instrumentation, (9 July 1998); doi: 10.1117/12.316831

SPIE.

Event: Astronomical Telescopes and Instrumentation, 1998, Kona, HI, United States

The Blue Channel of the Keck Low Resolution Imaging Spectrometer

James K. McCarthy[a,b], Judith G. Cohen[a,b],
Brad Butcher[a], John Cromer[b], Ernest Croner[b], Bill Douglas[b], Rich Goeden[a],
Tony Grewal[a], Barry Lu[a], Hal Petrie[b], Weng Tianxiang[a], & Bob Weber[b]

[a]Department of Astronomy and [b]Palomar Observatory
California Institute of Technology, Mail Code 105-24, Pasadena, CA 91125 USA

AND

Donald Koch[c] & J. Michael Rodgers[c]

[c]Optical Research Associates, 3280 E. Foothill Blvd., Pasadena, CA 91107 USA

ABSTRACT

This paper summarizes the optical, mechanical, electrical, and software design of LRIS–B, the blue channel of the Keck Low Resolution and Imaging Spectrograph. The LRIS–B project will shortly be completing the existing LRIS instrument through the addition of dichroic beamsplitters, grisms to disperse light on the blue channel, broad-band u, B, and V photometric filters, a blue and near-UV transmitting camera lens, and a large format blue-sensitive CCD detector. LRIS–B will also introduce piezoelectric xy-actuation of the CCD detector inside its Dewar, in order to compensate for flexure in the existing instrument; ultimately the red-side CCD detector will be similarly equipped, its PZT xy-stage being independently programmed. The optical design of the LRIS-B camera uses only fused silica and calcium fluoride elements, and includes a decentered meniscus element to compensate for coma introduced by the LRIS off-axis paraboloid collimator. The design of the blue channel grisms have been optimized for maximum blaze efficiency, the highest dispersion grism having a groove density of 1200 gr/mm. Optical elements not in use at any given time will be stowed in carousels externally mounted to the instrument sidewalls. The entire instrument is designed to permit remote operation.

1. INTRODUCTION

The Low Resolution Imaging Spectrometer (LRIS) for the Keck I Telescope is a highly efficient Cassegrain instrument built at Caltech under the direction of Profs. J.B. Oke and J.G. Cohen.[1,2] LRIS was a 4-year, $3.4M effort and was delivered to the Keck Observatory in May, 1993. Then followed a 2-year effort led by Cohen to improve the on-telescope reliability of the instrument and to isolate the CCD detector system from external noise sources surrounding LRIS at Cassegrain on Keck. However, the funds available initially were sufficient to build the instrument with only the red side of the dual beam system originally conceived by Miller[3] and Oke & Cohen,[4] and the multi-fiber-optic mode originally envisaged was never built. In early 1995 we were awarded $1.6M for LRIS–B, a project to complete LRIS by adding the blue channel dispersers and filters, blue camera optics and detector, and the dichroic beamsplitters necessary to convert the existing instrument into a double spectrograph.

When commissioned later this year, LRIS–B will immediately double the number of spectral resolution elements available with LRIS by dividing the wavelength range between the red and blue dispersing elements, cameras, and CCD detectors. Hence for low dispersion spectroscopy, the addition of the blue channel will permit an increase in dispersion by approximately 2× without any decrease in wavelength coverage. At higher dispersion, the blue channel will enable two selected wavelength regions to be observed instead of just one, increasing the total number of diagnostic spectral lines which can be studied in a given exposure time. Furthermore, the blaze wavelengths of the red and blue dispersing elements can be optimally selected independently (see Oke[5] for a discussion of the efficiency advantages of a double spectrograph). In imaging mode, two photometric bandpasses can be measured simultaneously, making more effective use of telescope time and at least partially mitigating the effect of thin cirrus on color indices. These efficiency benefits of a blue second channel would exist even if the wavelength coverage of the present red channel were complete.

Part of the SPIE Conference on Optical Astronomical Instrumentation • Kona, Hawaii • March 1998
SPIE Vol. 3355 • 0277-786X/98/$10.00

The existing LRIS–Red camera[6,7] includes optical glasses which become opaque in the near-ultraviolet. Therefore wavelengths $\lambda \leq 3800$ Å are currently unobservable with LRIS. With a design wavelength range of 3100 Å to 5500 Å, the LRIS–Blue channel will enable spectra and images to be obtained with maximum efficiency down to the atmospheric cutoff. Its optical materials, CCD detector, and anti-reflection coatings have been optimized for work in the blue and near-UV. It should also be noted that the atmospheric transmission in the near-ultraviolet at 13,800 ft. elevation is very high. Measurements[8] made at the Canada-France-Hawaii Telescope indicate that at 3200 Å the extinction is 0.82 mag/airmass, and it is below 0.50 mag/airmass for wavelengths longward of 3400 Å. Thus high sensitivity in the near-ultraviolet can be achieved with the Keck I Telescope, and there are many important scientific problems which LRIS–B will allow us to address in the near-UV for the first time.

2. OPTICAL DESIGN

The Keck I 10 m Telescope is a Ritchey–Chrétien design, having a focal ratio of f/15 and a curved focal surface whose radius is 2.14 m. The LRIS instrument images a 6 arcmin (Y) by 8 arcmin (X) multi-slit field-of-view which is centered 8 arcminutes off-axis in the dispersion (Y) direction. The optimum collimator design was found to be an off-axis paraboloid whose optical axis was coincident with the optical axis of the telescope, since the center of curvature of the Cassegrain focal surface and the center of curvature of the collimating mirror (focal length 2.0 m) were then nearly coincident. Figure 1 shows a YZ cross-section of the LRIS–Red and –Blue optical systems.

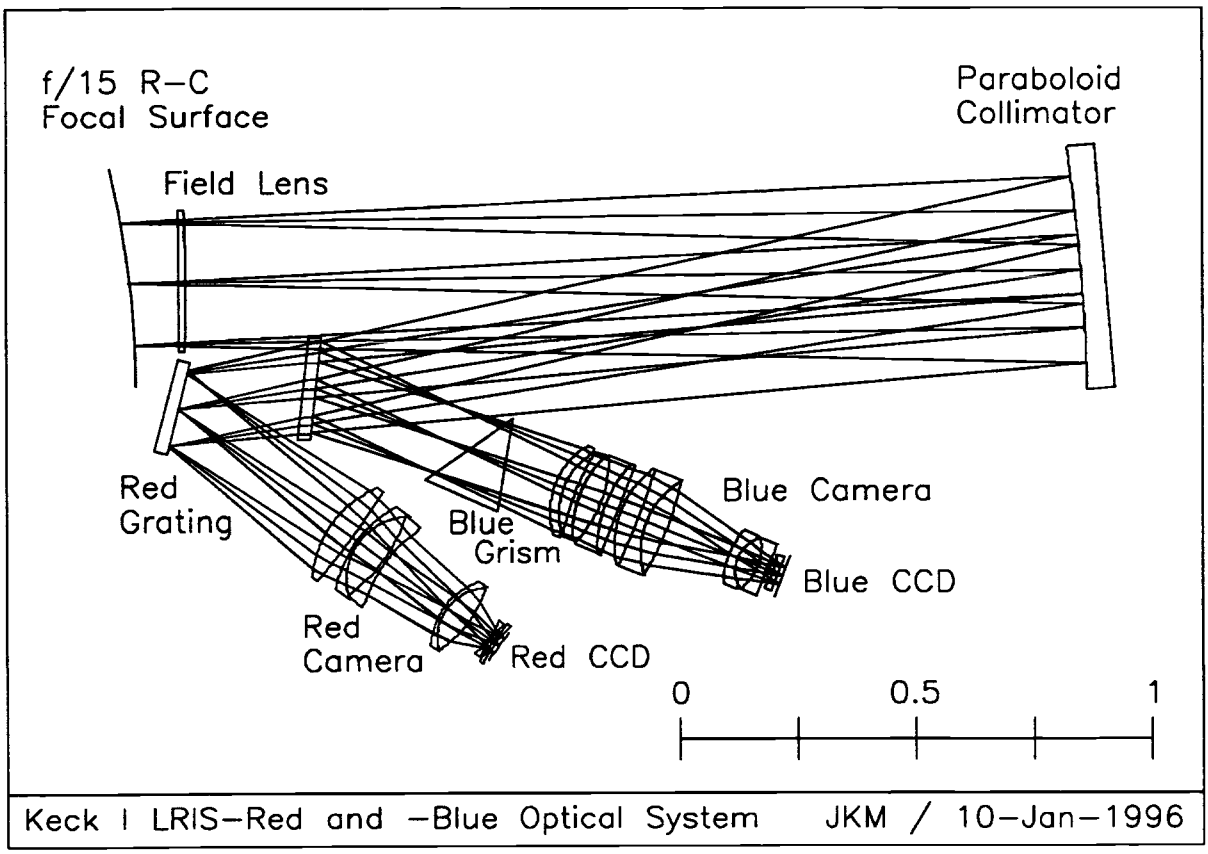

Figure 1. The LRIS–Red and –Blue optical systems shown in cross-section. The dichroic beamsplitter, inserted in the parallel beam between the collimator and the red grating, divides the collimated white light into red (transmitted) and blue (reflected) beams; note that the dichroic occults the lower edge of the incoming field. The blue grism is removed from the beam for imaging, while the red grating is replaced by a plane mirror. Filters (not shown) may be inserted into the parallel beams immediately before each camera. The bar shows a 1-meter scale.

2.1. The Blue Camera

As part of the LRIS–B Phase A study, Dr. J. Michael Rodgers of Optical Research Associates (ORA) designed candidate proof-of-concept camera lenses[9] for LRIS–B offering high performance (*i.e.*, low distortion, 80% encircled energy diameters less than 20 μm, fast 10-inch effective focal length, *etc.*) over the 3100 – 5500 Å bandpass of greatest importance for the blue side. Since that time, it was decided to lengthen the blue camera EFL to 12-inches (matching the red side) and to revisit the optical design of the blue camera including the as-built Keck I telescope and existing LRIS field lens and collimator optical parameters in the Code V design file. We felt this was important because, *e.g.*, the low distortion spec on the blue camera would be inappropriate if distortion were dominated by the upstream telescope and collimator. A further objective was to decrease the total path length through fluorite in order to maximize the total 3100 Å transmission, estimated at 70% in the original design based on a CaF_2 transmission[13] of 97.2% per inch at $\lambda = 3100$ Å. Later inquiries with Optovac revealed that, for low levels of cerium impurity, the bulk transmission of CaF_2 may be considerably higher,[14] up to 99.75% per inch at $\lambda = 3100$ Å.

The optical prescriptions of the as-built telescope and LRIS field lens and collimator are given below in Table 1, with the Keck I telescope data courtesy of Jerry Nelson,[10] the LRIS field lens and collimator data from Harland Epps[11] (design data) and Bev Oke[12] (as built data), and the dichroic tilt and LRIS collimator focus determined by our Code V raytrace.

Table 1: As Built Keck-I and LRIS Optical Design Prescription (mm)

Surface	Radius	Thickness	Material	Aperture	Notes
1	−34974.000	−15394.985	Refl.	10949.00	Keck I primary ($k = -1.003683$)
2	−4737.916	15394.985	Refl.	1499.42	Keck I f/15 sec ($k = -1.644326$)
3	∞	2499.965	Airspace	950.00	Distance behind primary vertex
4	−2144.014	76.200	Airspace	950.00	Curved f/15 focal surface
5	−10242.804	14.224	SiO_2	366 × 269[a]	LRIS field lens[b]
6	−4036.060	1921.577	Airspace	366 × 269[a]	LRIS field lens[b]
7	−4009.136	−1654.243	Refl.	543.56[c]	LRIS collimator ($k = -1.000$)
8	∞	287.770	Refl.	196.85[d]	Dichroic mirror[e,f]
9	∞	254.000	Airspace	148.09	Collimator pupil

[a] Aperture offset by $\Delta y = 305.3$ mm.
[b] Optical axis offset by $\Delta y = 278.511$ mm.
[c] Aperture offset by $\Delta y = 315.3$ mm.
[d] Aperture offset by $\Delta y = 82.9$ mm.
[e] Dichroic tilted by $\theta = -6.606°$.
[f] Optical axis rotated by $\theta = -21.900°$.

Including these foreoptics, the $15 - 20$ μm image diameters of the Phase A blue camera lens designs increased to $35 - 50$ μm (0.31 – 0.45 arcsec, comparable to the collimator + red camera) image diameters, largely dominated by coma from the LRIS off-axis paraboloid collimator. Because of the off-axis nature of the LRIS collimator and off-axis field, this coma aberration is all of the same sign and roughly the same magnitude. Therefore, the final blue camera lens design by Donald Koch at ORA now includes an aspheric meniscus first element which is *decentered* (by a mere 0.45 mm) to introduce coma opposite in sign to that introduced by the LRIS collimator, giving zero coma in the center of the LRIS field. The remaining on-axis lens elements of the camera are then able to cope with the (small) coma residuals increasing away from field center. The decentering of the meniscus does introduce a small tilt (less than 10 arcmin) to the focal plane, and optically both the focal plane (CCD) and field flattener (Dewar window) may be tilted as a unit. The final blue camera design (cross-section shown in Figure 1 above, and listed in Table 2) yields image diameters in the range $20 - 30$ μm (0.18 – 0.27 arcsec), including the Keck I Telescope + LRIS field lens and collimator.

Note that, with the exception of the aspheric first surface of the decentered front meniscus (maximum aspheric deviation = 196 μm; fabricated by R. Mathews Optical Works), all remaining blue camera lens elements have spherical surfaces (fabricated by Harold Johnson Optical Laboratory). Since all the LRIS–B camera lens elements are either fused quartz (Corning 7940 supplied by Advanced Glass Industries) or calcium fluoride, the near-UV transmission of the final anti-reflection (AR) coated LRIS–Blue camera lens system is expected to be very high (*i.e.*, over 90% at $\lambda = 3100$ Å). The CaF_2 material used for the blue camera is Optovac's low-cerium-impurity "UV Excimer Laser Grade" crystal. The "cemented" elements will be coupled with a fused silica index matching fluid (Cargille 50350).

Table 2: Final LRIS–Blue Camera Optical Design Prescription† (mm)

Surface	Radius	Thickness	Material	Aperture	Notes
9	∞	254.000	Airspace	148.09	Collimator pupil
10	159.395	20.000	SiO_2	203.20	Aspheric[a], Element decentered[b]
11	−150.786	26.847	Airspace	183.01	Element decentered[b]
12	562.258	11.000	SiO_2	184.15	First of cemented quartet
13	228.703	48.362	CaF_2	203.20	Second of cemented quartet
14	−244.113	11.000	SiO_2	203.20	Third of cemented quartet
15	−251.417	29.446	CaF_2	212.72	Fourth of cemented quartet
16	−36814.902	10.037	Airspace	212.72	Gap between quartet & triplet
17	201.282	39.478	CaF_2	215.90	First of cemented triplet
18	−2354.677	20.000	SiO_2	215.90	Second of cemented triplet
19	175.230	45.733	CaF_2	206.37	Third of cemented triplet
20	−586.005	142.917	Airspace	206.37	Gap between cemented triplets
21	168.881	20.000	SiO_2	139.70	First of cemented triplet
22	71.580	45.481	CaF_2	111.12	Second of cemented triplet
23	−116.528	20.000	SiO_2	111.12	Third of cemented triplet
24	385.725	15.685	Airspace	98.42	Airspace for shutter & focus
25	−112.112	10.000	SiO_2	88.00	Field flattener / Dewar window[c]
26	∞	11.000	Vacuum	88.00	Inside of CCD Dewar[c]
27	∞	0.000	CCD	88.00	Focal Plane[c]

†Note: All radii and thicknesses at operating temperature of +2° C.
[a] $k = -1.000$, $A = 2.26 \times 10^{-5}$, $B = 6.02 \times 10^{-8}$, $C = -1.42 \times 10^{-11}$, $D = 1.07 \times 10^{-12}$
[b] Element decentered by $\Delta y = 0.448$ mm.
[c] Surface tilted $\theta = 0.157$ degrees about vertex of surface 25 to compensate for decenter.

2.2. Grisms

The dispersing elements for the LRIS blue channel are grisms, four of which have been built for first light, and the on board grism changer (§3) will have capacity for six. To work efficiently down to the 3100 Å atmospheric cutoff, the grism substrate prisms are made of Corning 7980 fused silica (supplied by Advanced Glass Industries, polished by Planar Optics) and the ruled surfaces were replicated by the David Richardson Grating Lab using their "UV Resin". A prioritized list was selected from among the available 6×8 inch master rulings on the basis of simple calculations[16] of blaze peak wavelengths and blaze profile shapes. Roughly speaking, these fell into two categories: (i) grisms with blaze peak wavelengths of $3300 - 3400$ Å, very near the atmospheric cutoff, where near-UV science programs unique to LRIS–B on Keck were likely to be the most photon-starved, and (ii) grisms with blaze peak wavelengths greater than 4000 Å, which provide generally high efficiency throughout the $3500 - 5500$ Å "blue" spectral region.

We sought to achieve the highest possible blaze efficiency for each of the LRIS–B grisms, in particular for high groove density rulings ($N \geq 600$ gr/mm) where conventional wisdom held that grism blaze efficiency is poor ($\eta_{\rm peak} \leq 0.50$), since "scalar" grating blaze theory no longer applies when the groove spacing becomes comparable to the wavelength of light. In a series of *Applied Optics* papers,[17–19] Prof. M. Nevière of the Laboratoire d'Optique Electromagnètique, Marseille University, has discussed his research into the application of electromagnetic theory to gratings, including the grism case. With Prof. Nevière working as a consultant, the electromagnetic theory was applied to the candidate LRIS–B grisms to optimize the incidence angle (α, the angle between the normal of the ruled face and the incident optical axis) of light onto the chosen grism rulings to maximize blaze efficiency at the wavelengths of interest. Table 3 below summarizes these results. The seventh column, λ Coverage, shows the wavelength range emerging from the grism within the $\pm 5.8°$ angular size of a $4096^2 \times 15\,\mu$m CCD in the focal plane of the 12-inch focal length blue camera. The eighth column, $\Delta\lambda$, is divided into two columns based on the two blaze peak wavelength categories above; the grism priorities (column 9) were assigned in order to provide a range in grism dispersion in each category. The prism apex angles in Table 3 were calculated in order either *(i)* to position the blaze peak near the center of the CCD (for the 150, 300, and 400 gr/mm grisms, allowing for possible multiple columns of entrance multi-slits) or else *(ii)* to locate light at the short wavelength limit on the edge of the CCD (for the 600 gr/mm and higher grisms).

Table 3: Optimized Parameters for LRIS-B Grisms

Gr/mm	Blaze Angle	Optimum α	Prism Apex	η_{peak}	λ_{peak}	λ Coverage	$\Delta\lambda$ (Å/0.8″ slit)	Priority
150	7°.33	8°.106	8°.33	87%	4500	2000 – 9900	19.1	8
300	17°.50	17°.132	20°.00	79%	5250	2500 – 8300	9.5	3
400	13°.90	14°.813	20°.00	81%	3350	2400 – 6000	5.8	2
632	22°.30	14°.153	33°.33	74%	3400	2950 – 5600	4.3	7
600	28°.70	32°.956	33°.33	73%	4200	3050 – 5550	4.0	1
830	30°.00	29°.079	42°.25	71%	3350	3000 – 4800	2.9	5
830[a]	34°.37	24°.016	41°.75	69%	3750	3000 – 4850	3.0	...
900[a,b]	43°.00	39°.800	44°.50	66%	4100	3900 – 5400	2.4	6
600[a,c]	47°.52	35°.487	57°.06	68%	3400	3000 – 4000	1.6	...
1200	46°.00	38°.457	57°.88	65%	3350	3000 – 4000	1.6	4

[a]These grisms would require custom master rulings by Milton Roy.
[b]This grism uses Milton Roy's "Resin A" and LF5 glass for $\lambda > 3600$ Å; all other grisms use Milton Roy's "UV Resin" and fused silica prisms for work down to $\lambda = 3000$ Å.
[c]This grism is used in $m = -2$ for higher dispersion; all others are used in $m = -1$.

2.3. Spectrum-Shifting Wedges

The wavelength range of each grism listed in Table 3 is relatively insensitive to grism tilt, and so the grism in use will be held fixed inside LRIS without tilt adjustment. To shift the spectral range towards longer wavelengths, it will be possible to insert thin fused silica wedges into the beam behind the grisms to accomplish half- and full-CCD-width spectrum shifts to the red. These wedges would be carried in "filter cells" and interchanged with the bandpass filters used for imaging on the blue side; the LRIS–B design layout calls for the blue filters to be located between the grism and the blue camera, which is also the ideal location for such a spectrum-shifting wedge. The alternative used in most transmission grating or grism instruments in which a spectrum shift is possible — namely, rotating the camera about an axis through the dispersing element — is far less desirable mechanically. Were both a filter (*e.g.*, for order separation with the $m = -2$ high dispersion 600 gr/mm grism) and a spectrum-shifting wedge required for a special purpose (*i.e.*, when for some reason the dichroic would not suffice for this purpose), these could be combined inside the same filter cell and inserted together for use.

No spectrum-shifting wedges are needed for the grisms planned for first light, since their blaze profiles are nicely accommodated by the CCD; the penalty of a half- or full-CCD-width shift in terms of grism blaze efficiency would be high for these grisms, sufficient to justify fabrication of a new grism over fabrication of a spectrum-shifting wedge.

2.4. Blue Filters

Filters used on the blue side of LRIS will be located immediately in front of the camera, in the parallel beam. Three filters are being fabricated for first light:

- A filter similar to Sloan "u", bandpass 3180 – 3800 Å, with peak transmission $\simeq$ 80%, comprised of 1 mm of Schott UG11, an interference coating to define the long wavelength edge of the bandpass, and a second interference coating for IR-blocking. This filter will be fabricated by Barr Associates.
- A filter similar to Johnson "B", bandpass 4000 – 4800 Å, with peak transmission $\simeq$ 80%, created using interference coatings on a filter glass substrate. This filter has been fabricated by Barr Associates.
- A Johnson "V" filter, bandpass 4900 – 6000 Å, with peak transmission $\simeq$ 80%, comprised of 3 mm of Schott GG495 and 2 mm of Schott BG18. This filter has been fabricated by Cosmo Optics.

The LRIS–Blue channel filters must have overall dimensions of 203.2 mm (8.000 inches) × 190.5 mm (7.500 inches) and may be up to 12 mm thickness (0.50 inches). Filters will be tilted by 6° to the optical axis of the blue camera. The fabrication of thin (*e.g.*, 1 mm) polished filter glass layers presents considerable challenges in this large aperture. The use of interference coatings to define the bandpass edges introduces some dependence on the incident angle, which varies across the field. However, simulations by Barr Associates have demonstrated that this field-dependent wavelength shift in the bandpass edges is small ($\Delta\lambda \leq 20$ Å) and will pose no problem for most work.

2.5. Dichroic Beamsplitters

The dichroic beamsplitters have an aperture of 204.5 mm × 213.4 mm (8.05 × 8.40 inches), and in order to minimize bow of the reflecting surface, they are 25.4 mm (1.00 inch) thick. The dichroics will be used at nominal angles of incidence and reflection of 15° to the surface normal, for a total deviation of the optical axis by 150° to the blue side.

- 4600 Å transition, allowing 3100 – 4600 Å to be recorded on the blue side at moderate resolution while 4500 – 6500 Å is recorded on the red side (*e.g.*, with a 1200 gr/mm grating having a 5000 Å blaze peak). A second red grating setting (6500 – 9000 Å) would nearly complete the wavelength coverage in the red, while typically a second exposure covering the same blue/UV wavelength region would be obtained for higher S/N.
- 5000 Å transition, for imaging to send the B filter bandpass to the blue side while simultaneously sending the V filter bandpass to the red side.
- 5577 Å transition, for lower resolution spectroscopy with 3100 – 5600 Å recorded on the blue side (*e.g.*, with the 400 or 600 gr/mm grisms) while 5500 – 10000 Å is recorded on the red side (*e.g.*, with the 300 gr/mm grating blazed at 6400 Å).
- 6800 Å transition, to allow a very low dispersion (large wavelength coverage) spectrum to be obtained with the blue side (*e.g.*, with the 300 or 150 gr/mm grisms) while, on the red side, higher dispersion is used over a smaller wavelength range (*e.g.*, 6800 – 10000 Å) in order to better separate the OH night sky emission lines.
- Mirror, to send all light to the blue side. Removing the dichroic from the beam would send all light to the red side of LRIS as happens at present.

These dichroic coatings have been designed and are being fabricated by ZC&R Coating Laboratory. The BK7 dichroic substrates, fabricated by Gould Precision Optics, were polished on two sides which are parallel to within ±5 arcsec. As pointed out by Oke,[2] this is necessary so that red light transmitted by the dichroic coating (*e.g.*, in the dichroic cross-over region), reflected by the AR-coated rear surface, and transmitted again by the dichroic coating, will be coincident with light reflected by the dichroic coating when imaged by the blue camera.

2.6. Red Side Imaging Fold Mirror

Currently, when the existing LRIS (red) instrument is used for imaging on one of the Keck Telescopes, the best images are obtained when the telescope's f/15 secondary mirror is purposely misaligned to introduce coma of opposite sign to that which originates in the LRIS paraboloid collimator in combination with the off-axis field of view. Since the LRIS–B camera will itself correct for collimator coma (see §2.1), the blue channel will adversely suffer from misalignment of the telescope secondary. In addressing this dilemma, we noted that:

- spectroscopic observations require the best images in the slit plane, and as such are adversely affected in both red and blue channels by telescope secondary misalignment;
- interior to LRIS, spectroscopy involves imaging the slit mask onto the CCD — on the blue side, spectrograph optical performance is improved by correcting collimator coma in the design of the camera — on the red side, telescope secondary misalignment cannot improve LRIS optical performance in spectroscopy mode;
- the LRIS field of view is off-axis and the Cassegrain instrument must rotate during exposures since the Kecks are alt-azimuth telescopes — therefore the direction of telescope secondary misalignment required to improve LRIS red channel imaging must change as LRIS rotates in the Cassegrain module.

Therefore we were reluctant to abandon the blue camera's coma correction in favor of the red channel solution involving telescope secondary misalignment. Since the current LRIS red channel only benefits from secondary misalignment in imaging mode, we commissioned ORA to investigate correcting LRIS collimator coma by replacing the flat imaging fold mirror in the red grating turret with one having an aspheric figure. Their design study[20] concluded that some benefit would indeed accrue from a Zernike surface figure on the red side imaging fold mirror. The region of best imaging moves closer to the center of the red CCD, the mean rms image diameter across the field decreases from 38.4 μm to 31.4 μm, and the worst images (those in the corners furthest off-axis) are significantly improved (from 59.4 μm to 38.3 μm in rms diameter). Fabrication of this non-rotationally symmetric aspheric mirror would be expensive, and so the decision whether to proceed is currently on hold pending successful demonstration of coma correction with the blue channel camera's decentered first element.

3. MECHANICAL DESIGN

The overall mechanical design of the Keck LRIS is described by Oke *et al.*[2] The mechanical design challenges presented to LRIS–B were nevertheless several. LRIS is physically one of the world's largest astronomical spectrographs to move on a telescope at the Cassegrain focus. As such, it is unfortunately susceptible to image shifts of a few CCD pixels (24 μm each) over the course of long exposures due to the changing forces acting on the instrument both from gravity and from the Cassegrain instrument module which carries LRIS and rotates it with respect to the Keck telescope. Our challenge is to add the blue channel to this instrument without making a bad flexure problem on the red side worse, and to minimize to the extent possible the flexure on the new blue side. A second mechanical design challenge originated from our desire to locate the blue channel grism as close to the pupil as possible to maximize throughput and minimize size (and cost) of the grisms as well as of the quartz/fluorite blue camera. We also wished to minimize the obscuration of the LRIS input field of view caused by the dichroic, its cell, and its transporting/mounting structures (see Fig. 1).

With regard to the flexure issues, we conducted an independent finite element analysis (FEA) of LRIS as built, which concluded that the instrument structure is in fact adequately stiff, both to support the added weight of the blue channel components without significantly increasing red channel flexure and to provide a stiff anchor for the blue channel optics mounts, particularly the dichroic. This conclusion, and the fundamental validity of our FE model, were later verified by the agreement between FEA simulation of flexure and experiment with a 200 lb. person standing on the LRIS instrument sidewall near the collimator cell; the predicted and observed flexure shifts (~ 0.2 pixel) for this experiment were in agreement to better than 20%. Our very detailed FE model also identified the red grating turret as likely the major contributor to the flexure present on the red side. To address whatever flexure may appear on the LRIS blue channel (and eventually, also on the red channel), we have developed the means to actively position the CCD detector in the camera focal plane using piezoelectric transducers (PZTs; see §4.2 below).

The optically optimum positions for the blue channel grism and filter brought these elements closer to the dichroic, ruling out the option (which would have been difficult to implement in any case, given other space constraints on LRIS) of stowing these optics inside linearly translating racks ("jukeboxes") on the instrument sidewalls as are the existing LRIS slitmasks and red channel filters. The conflicts arose from the space required for translation. Instead, we have designed rotating carousels for the blue channel grisms, filters, and dichroics. Besides requiring less physical volume, the rotating carousels are balanced around their axes and will not require lifting the mass of optics and cells against gravity in certain orientations. Originally one dichroic carousel and one combined grism/filter carousel were planned; we have since opted for separate grism and filter carousels located on opposite LRIS sidewalls (see Fig. 2).

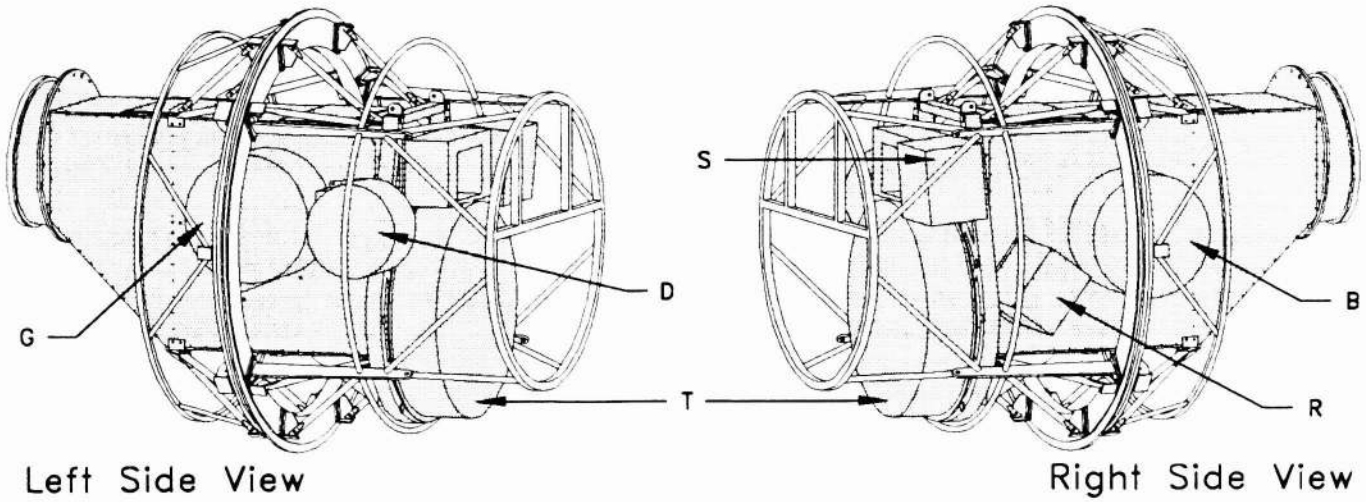

Figure 2. Left and right side views of the LRIS instrument (shaded), supported by struts inside the large mounting ring which surrounds the spectrometer at its center of gravity. Light enters through the upper middle section of the forward guard ring. The blue grism [G] and dichroic [D] carousels can be seen attached to the left sidewall (the dichroic carousel being elevated to clear the red grating turret [T] mount), and the blue filter [B] carousel can be seen on the right side with the slitmask [S] and red filter [R] jukeboxes.

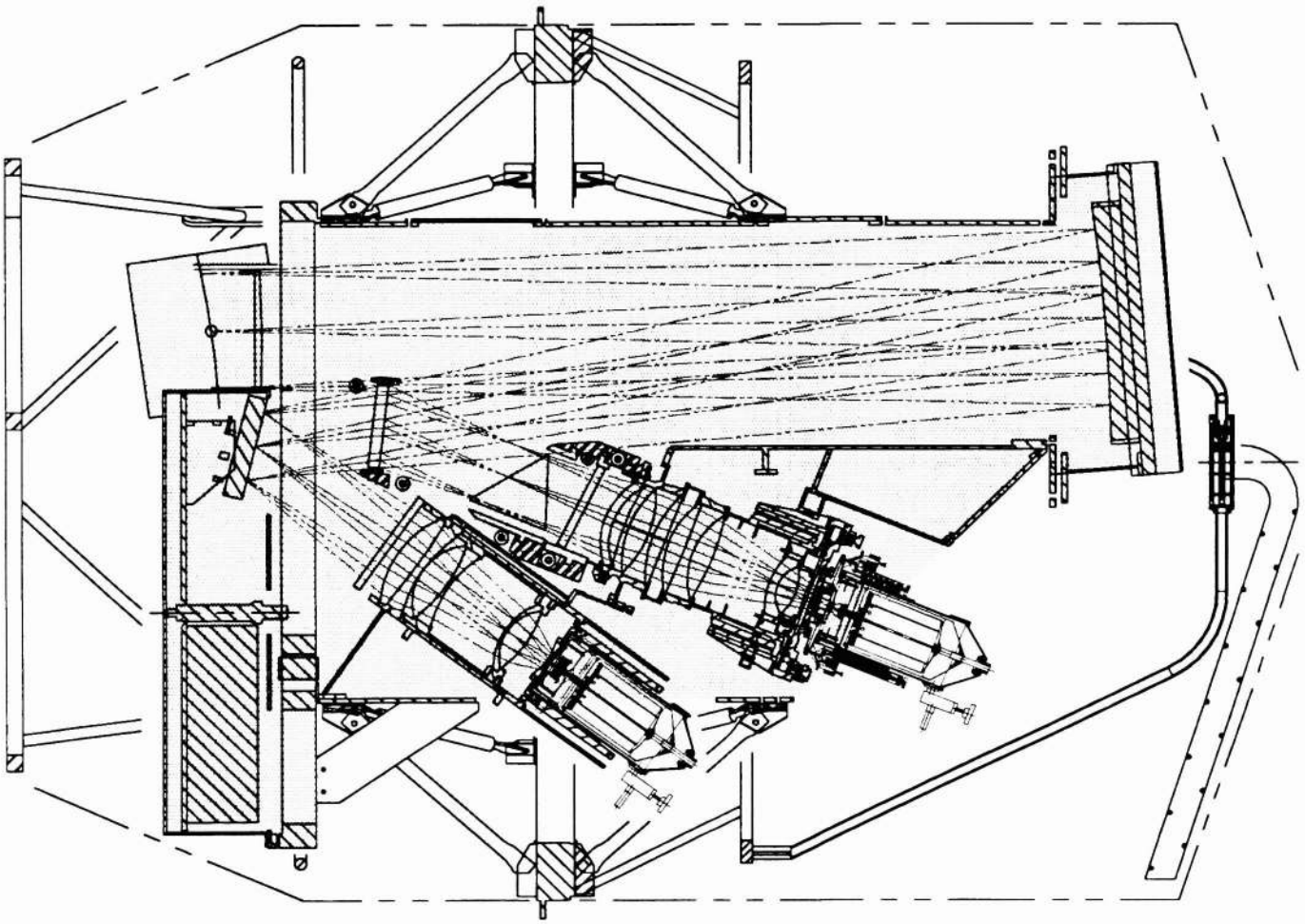

Figure 3. A cross-sectional view of the LRIS instrument (shaded) showing both the red and blue channels. This view, facing the right side of Fig. 2, has the same orientation and nearly the same scale as Fig. 1 (the as-built optical raytrace data from Code V has been replicated in 3-D inside our AutoCAD model by a utility program written in AutoLISP). The red and blue camera bulkheads shown in the lower half of this figure have been redesigned from the originals, which will be replaced when the blue channel is installed. The dichroics and blue channel filters and grisms are pulled into place by dual leadscrew drive assemblies, within rails perpendicular to the plane of this figure.

The camera lens cell for LRIS–B is shown installed in Fig. 3 and in detail in Fig. 4. Its mechanical design is a derivative of the cells for the Keck LRIS red camera[1] and the Hale Double Spectrograph red camera,[21] having more in common with the latter. The lens elements are held radially at their edges by delrin dowels pressed into holes drilled axially around the inside circumference of the 416 stainless steel cells; the partly-exposed semi-cylinders of delrin are then bored all at once to match the lens element O.D. Not only does this design eliminate metal-to-glass contact, the outward expansion with temperature of the 416 stainless cell relative to the glass is largely compensated for by the inward expansion of the cylindrical delrin pad contacts. Axially, the lens groups are registered against metal lips at one end with kapton shims to protect the glass, and they are held in place by an O-ring lip pressing against the other end of the group. The detailed design of the LRIS–B camera lens cell was complicated by the need to seal the inner circumference because the lens elements are joined together with a fluid couplant. Neoprene O-rings were tested and found to be compatible with the Cargille fused silica index matching fluid used.

A screw-adjustable decentering is provided for the front meniscus element relative to the rest of the camera, in order to achieve the coma correction described in §2.1 above. The associated tilt of the CCD detector and field-flattener/Dewar-window (*i.e.*, the entire CCD Dewar) is provided via adjustments in two dimensions rather than one, as a more convenient way to fine tune the CCD levelling first done inside the vacuum Dewar during assembly.

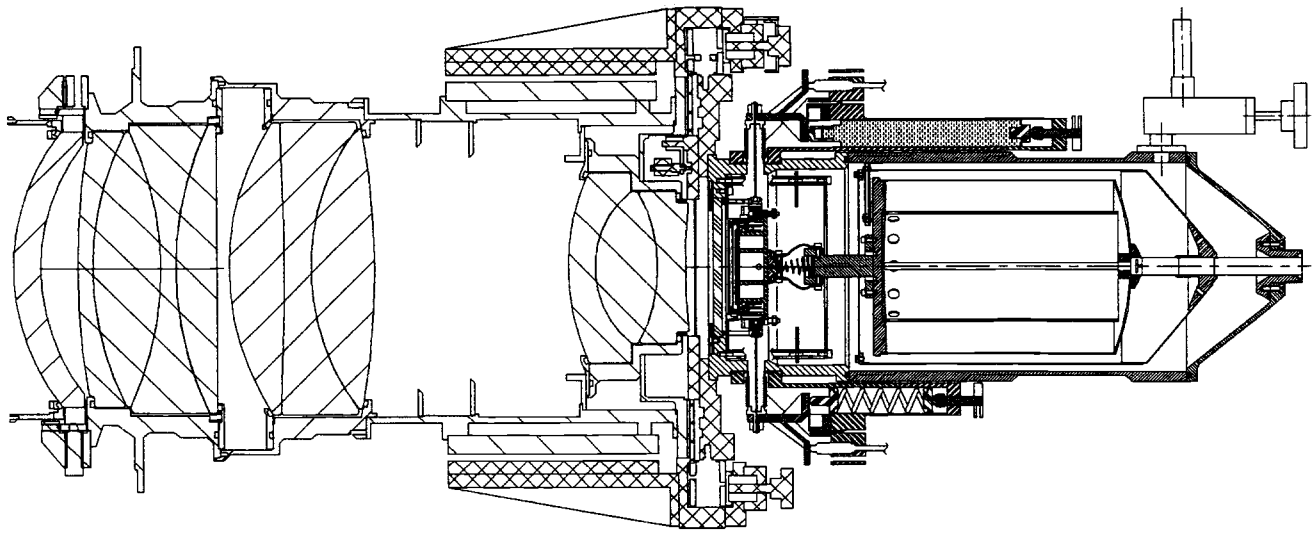

Figure 4. Cross section of the LRIS–B camera lens cell (left; coarsely hatched) and the active piezo-xy CCD Dewar (right; finely hatched). The interface between the two provides for focus adjustment using four cross roller linear slides (center; parts which move relative to the camera barrel are shown cross-hatched). For illustration purposes, the slides have been rotated around the optical axis by 45° from actual so that two appear in this section. One axis of the gimbal mechanism for CCD tilt adjustment and one axis of the CCD piezo-xy translation system are also shown (orientation same as actual). The liquid nitrogen Dewar depicted is a standard IR Labs model ND-5, although the custom ND-5 Dewar to be used is "stretched" axially for increased LN2 capacity.

4. CCD DETECTOR SYSTEM

4.1. CCD Detector and Electronics

The CCD detector to be used initially on the LRIS–Blue channel is an engineering grade SITe 2048 × 2048 array of 24 μm pixels, having one low noise on-chip amplifier (output "C", readnoise 4.8 e^- r.m.s.)†. In addition, this device has SITe's UVAR-coating, achieving 30–40% quantum efficiency (QE) over the 3000 – 4000 Å wavelength region. The pixel size and format is therefore identical to that currently in use on the LRIS–Red channel. Future upgrades to 4096 × 4096 arrays of 15 μm pixels are planned for both the red and blue channels for still greater quantum efficiency, slightly larger field and wavelength coverage, and improved image sampling of the best seeing achieved with the Keck telescopes. On the red channel, the improved far red response and reduced QE-fringing of deep depletion CCDs makes these the obvious upgrade choice, likely in the form of a 1 × 2 mosaic of 4096 × 2048 buttable devices. On the blue channel, the 4096^2 upgrade is expected to employ a monolithic 4096^2 device (dubbed "BIG CIT" when designed by J. Janesick) custom fabricated for Caltech in early 1996 by Loral Fairchild (Milpitas, CA). Fourteen wafers were produced, of which seven are candidate science-grade devices; the rest typically have DC shorts on only one half of the array and are therefore useful as engineering test devices. Currently these wafers are being thinned at the Steward Observatory CCD Lab (M. Lesser), with the goal being to produce one engineering grade thinned device first, followed by as many thinned science grade devices as possible (target is five). The $\geq$ 80% near-UV quantum efficiencies achieved by Lesser[22] make this approach attractive to upgrade both LRIS–B and Keck HIRES.

Following our standard practice at Palomar Observatory[23,24] and on the LRIS–Red channel, the CCD off-chip preamplifiers are housed inside the Dewar on an uncooled circuit board surrounding the cold CCD container. This keeps wire lengths to a minimum and provides a shielded environment for the low noise preamps, of which there are two in the LRIS design. Low pass filtering of the CCD clock lines also occurs on the circuit board inside the Dewar. Exterior to the Dewar, the remaining CCD controller electronics for LRIS–B are the Leach "Generation I" design.[25] On the blue channel, we are incorporating the new "dual analog" video signal chain board and adopting Leach's power conditioning board (which was introduced only after the red channel controller had been built with custom electronics for those power-on functions) and VME interface.

†The output amplifier ("D") at the opposite end of the lower serial register has approximately 20 e^- readnoise, so that dual-amplifier readout is ruled out for most science integrations but will still be useful for faster readout of setup and alignment images.

4.2. Active Flexure Compensation

As part of the LRIS–B project, McCarthy[26] proposed to implement active flexure compensation by moving the CCD detectors within their liquid nitrogen (LN_2) Dewars. Other approaches under consideration at the time (*e.g.*, moving the spectrograph collimator mirror, as suggested to Oke by Walker[27,28]) would influence both the red and blue channels together, requiring an additional active component (*e.g.*, the dichroic beamsplitter) to compensate for different motions in the red and blue channels — were the blue channel to prove relatively immune from flexure (*e.g.*, originating in the red grating turret), this would then involve introducing a large [red side] flexure correction at the collimator which would then need to be removed at the dichroic. In contrast, the active CCD approach would permit two identical systems to be built (one for the red camera CCD, and one for the blue camera CCD) and simply programmed to move independently under computer control to correct only the flexure experienced by that channel alone. It was also apparent, meanwhile, that the same CCD motion capability would — if operated at a sufficiently high frequency — stabilize direct images in the presence of blurring caused by wind shake, telescope tracking and guiding errors, and (at least on smaller telescopes) wavefront tilt caused by the earth's atmosphere (see Tonry *et al.*[29] for an excellent discussion of atmospheric image motion compensation; high speed imaging experiments[30] at Keck have shown little or no correlated image motion, however).

The proposed piezoelectrically active CCD Dewar has been designed and built,[31] and is shown in cross-section in Fig. 4. The long cylindrical PZTs (Physik Instrumente model number P–844.60, one for each axis, x and y) are mounted axially alongside the Dewar with return springs diametrically opposite. L-shaped lever arms convert the axial PZT (or spring) expansion into radially outward (tension) force on thin stainless steel wires passing through bellows radially into the center of the CCD Dewar. The bellows permit mechanical motion of the lever arms and wires while maintaining the vacuum inside the Dewar. Surrounding the CCD mount in the center of the Dewar are mechanical flexures in x and y which allow the CCD to translate in response to the net tension force on the four wires. For 90 μm of total PZT expansion ($0-100V$), the resulting CCD motion is $\pm 150\,\mu$m (± 6 pixels) on each axis. Paddles on the outsides of the L-shaped lever arms contact LVDT sensors (two per axis) whose net translation signal provides electrical feedback to the PZT controller (Physik Instrumente model number P–925.306) in such a way that common-mode changes (both levers moving inward, or both moving outward) properly do not register as a change in CCD position. Included in our design are adjustments to set the mid-stroke expansion of the PZT at the mid-stroke of the CCD stage flexure travel, and to set the desired wire tension via compression of the return spring.

Our intent is to command the CCD xy position "open loop" on the basis of a software lookup table which maps the blue channel flexure. If successful in removing LRIS flexure by tracking it with CCD motion, a duplicate system would be introduced on the red channel and commanded from a second [different] lookup table. While LRIS–Red channel flexure measurements do behave predictably without significant hysteresis, our active CCD design incorporates a photodiode quad cell in the lid of the moving CCD container, out of the input field from the LRIS slitmask imaged onto the CCD array. Conceivably an arc line source could be provided alongside the LRIS slitmask or field lens which would illuminate the photodiode quad cell in the camera focal planes, for optically "closed loop" flexure compensation. However, we are confident the software lookup table "open loop" implementation will provide satisfactory flexure compensation.

5. INSTRUMENT ELECTRONICS

Each of the blue channel optics carousels will be stepper-motor driven, with absolute encoders providing position information on demand. One stepper motor will also drive the pair of leadscrews which pull the optic from the carousel and into position in the LRIS beam. Motions of each carousel and corresponding leadscrew drive are interlocked by design, as they share one stepper motor controller+driver which is multiplexed to power only one of the motors at any given time. Position sensors (*e.g.*, Hall effect sensors) will confirm that leadscrew travel in either direction has been successfully completed, and that carousel rotation has stopped at one of the indexed optic positions. The blue channel will introduce an ethernet terminal server on board the instrument in order to handle RS-232 serial communication with each of the three stepper motor controllers (one each for the dichroic, blue grism, and blue filter carousels, with the lowest duty cycle optic — the dichroic — also multiplexed to drive the CCD focus motor) and the absolute encoders.

Currently the LRIS instrument electronics are attached to cooled plates arrayed on the inside circumference of the large ring mounted behind the main instrument mounting ring (see Figs. 2 and 3). To accomodate the additional LRIS–B electronics and improve the heat removal efficiency, the instrument electronics will be repackaged into a cooled enclosure to be mounted on that ring. Improved serviceability should result from the new electronics layout.

6. SOFTWARE

The software used to operate the LRIS–Blue channel has a large inheritance from that used to operate the existing LRIS–Red and HIRES optical instruments at Keck Observatory (*e.g.*, tools to control CCD exposure, image display, keyword libraries to record instrument status and initiate configuration changes, communication interfaces to the telescope control system, *etc.*). There are, however, several new software capabilities required by LRIS–B. These are: (a) dual CCD camera control and readout capability; (b) open loop PZT flexure compensation via software lookup table; (c) operation to select optics from "carousels" as distinct from linearly translating "jukebox" racks; and (d) an expanded graphical user interface (GUI) to the astronomer incorporating both the red and blue channels of LRIS. Work is progressing in each of these areas, and the new GUI is shown in Figure 5.

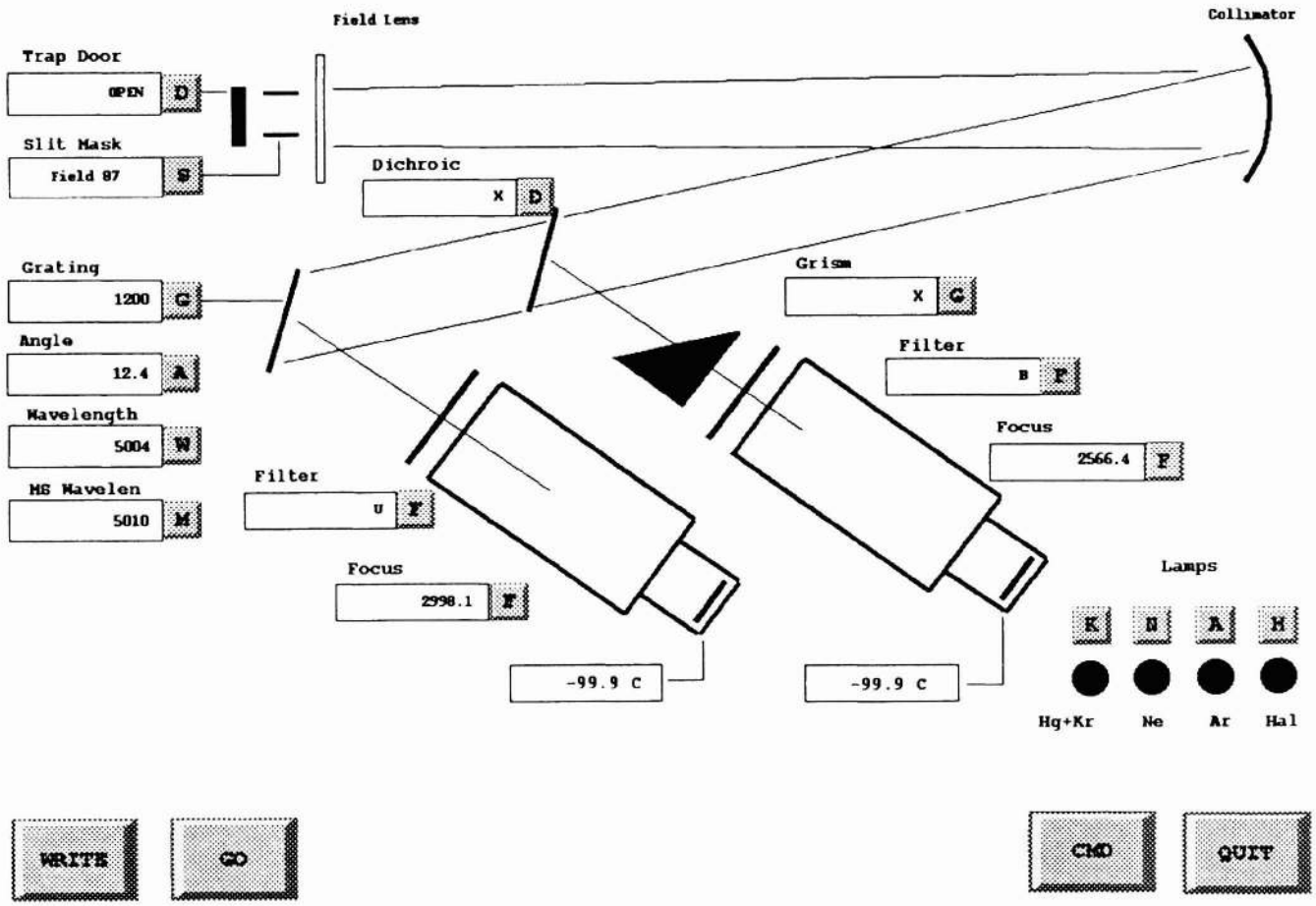

Figure 5. The XLRIS graphical user interface for control of all instrument functions, both blue and red. The small grey buttons activate pop-up menus with which the astronomer may select from among the available optics, set camera focus, or set the tilt of the red grating. The large grey buttons along the bottom are used to create or invoke setup "scripts" which initiate numerous configuration changes in parallel.

CCD readout and stepper motor control are each performed by CPU's configured in VME crates running the VxWorks real time operating system. These communicate via fiber optic links to the Leach CCD controllers, and via RS-232 serial (on the red channel) or ethernet terminal server to RS-232 (on the blue channel) links to the API motor controllers and encoders. The capacity of the terminal server is sufficient to handle both blue and red channel control in the future. A local ethernet connects each of the VME crates to the main Sun SPARCstation instrument computer, which runs the X-windows graphical user interfaces needed by the astronomer for instrument status control (xlris; Fig. 5), CCD exposure time monitoring and control (xpose), CCD data display and quick-look analysis (figdisp), and added to this list will be PZT flexure compensation monitoring and control.

ACKNOWLEDGMENTS

The LRIS–B project was funded by the California Association for Research in Astronomy, and it is a pleasure to acknowledge the Keck Foundation and the late Howard Keck for the gift which made the W.M. Keck Observatory possible. We also wish to thank the members of the LRIS–B design review panels (Bev Oke, chair, Tom Bida, Harland Epps, Jim Gunn, Gary Hill, Frank Melsheimer, and Jerry Nelson) for their insightful comments.

REFERENCES

1. Oke, J.B., Cohen, J.G., Carr, M., Cromer, J., Dingizian, A., Harris, F., Lucinio, R., Labrecque, S., Schaal, W., and Southard, S. Jr., 1994. *Proc. S.P.I.E.*, v. **2198**, p. 178.
2. Oke, J.B., Cohen, J.G., Carr, M., Cromer, J., Dingizian, A., Harris, F.H., Labrecque, S., Lucinio, R., Schaal, W., Epps, H., and Miller, J., 1995. *P.A.S.P.*, v. **107**, p. 375.
3. Miller, J., 1987. In *Instrumentation for Ground Based Optical Astronomy, Proc. Ninth Santa Cruz Summer Workshop*, L. Robinson, ed., p. 153.
4. Oke, J.B., and Cohen, J.G., 1989. LRIS funding proposal to CARA.
5. Oke, J.B., 1987. In *Instrumentation for Ground Based Optical Astronomy, Proc. Ninth Santa Cruz Summer Workshop*, L. Robinson, ed., p. 172.
6. Epps, H.W., 1988. In *Proc. ESO Conf. on Very Large Telescopes and Their Instrumentation*, M.-H. Ulrich, ed., p.1157
7. Epps, H.W., 1990. In *Proc. S.P.I.E.*, v. **1235**, p. 550.
8. Alloin, D., Boulade, O., and Vigroux, L. 1994 *CFH Info. Bulletin*, v. **11**, p. 812.
9. Rodgers, J.M., and McCarthy, J.K., 1994. *Proc. S.P.I.E.*, v. **2198**, p. 1096.
10. Nelson, J., 1994. *Keck Observatory Technical Note 163*, Revision 5, dated 23 November 1994.
11. Epps, Harland W., 1990. *LRIS Collimator and Field Lens Design and Raytrace, Final*, computer output dated 1 June 1990 (on file at CARA).
12. Oke, J.B., and Cohen, J.G., 1993. *The Low Resolution Imaging Spectrometer: Manual of Operations*, 11 January 1993 edition.
13. Standard CaF_2 transmission at $\lambda = 3100$ Å as quoted by Harshaw.
14. Harrington *et al.* 1978, *Appl. Optics*, v. **17**, p. 1541.
15. Brown, Wm., 1995. Private communication.
16. Traub, W.A., 1990. *J.O.S.A.–A*, v. **7**, p. 1779.
17. Loewen, E.G., Nevière, M., and Maystre, D., 1977. *Appl. Optics*, v. **16**, p. 2711.
18. Nevière, M., 1991. *Appl. Optics*, v. **30**, p. 4540.
19. Nevière, M., 1992. *Appl. Optics*, v. **31**, p. 427.
20. Chrisp, Michael, and Rodgers, J. Michael, 1996. *Optical Research Associates Preliminary Design Study*, 8 July 1996.
21. McCarthy, James K., and Weber, Robert W., 1995. "A New Red Camera for the 200-inch Double Spectrograph," in *Annual Report of the Palomar Observatory 1995*, ed. J. Westphal.
22. Lesser, M. 1994. *Proc. S.P.I.E.*, v. **2198**, p. 782.
23. J.E. Gunn and J.A. Westphal, 1981. *Proc. S.P.I.E.*, v. **290**, p. 16.
24. J.E. Gunn, E.B. Emory, F.H. Harris, and J.B. Oke, 1987. *P.A.S.P.*, v. **99**, p. 518.
25. Leach, Robert, and Beale, Frank, 1990. *Proc. S.P.I.E.*, v. **1235** (Tucson 1990), p. 284.
26. McCarthy, James K., & Cohen, J.G., 1994. LRIS–B funding proposal to CARA.
27. Walker, D., Dryburgh, M., & Bigelow, B., 1992. "Control of Flexure in Gemini Instrumentation", *Design Study Report* commissioned by Gemini Tucson office, unpublished.
28. Walker, D.D., Radley, A.S., Diego, F., Charalambous, A., Dryburgh, M., & Bigelow, B.C., 1994. *Proc. S.P.I.E.*, v. **2198**, p. 1083.
29. Tonry, J.L., Burke, B.E., and Schechter, P.L. 1997. *P.A.S.P.*, v. **109**, p. 1154.
30. Dekens, F., Kirkman, D., Chanan, G.A., Mast, T.S., Nelson, J.E., Illingworth, G., & Wizinowich, P.L., 1994. *Proc. S.P.I.E.*, v. **2201**, p. 310.
31. McCarthy, J.K., Lu, B.W., Butcher, B.A., Behr, B.B., Jensen-Grey, S., Stubbs, C., Jim, K., & Brown, Y. 1998. *P.A.S.P.*, in preparation.